J. Geodynamics Vol. 15, No. 1/2, pp. 59–83, 1992
Printed in Great Britain.

0264-3707/92 $5.00+0.00

FROM LATEST MIOCENE THRUSTING TO QUATERNARY TRANSPRESSION AND TRANSTENSION IN THE INTERANDEAN VALLEY, ECUADOR

A. TIBALDI and L. FERRARI

Dipartimento di Scienze della Terra, Università di Milano, Via Mangiagalli 34, 20133 Milano, Italy

(Received 4 June 1991)

Abstract—Field studies of folds and striated fault planes were carried out in the Interandean Valley (IV) of Ecuador, a NNE–SSW elongated depression lying between the Cordillera Occidental and the Cordillera Real. Four tectonic events were recognized: (a) at the end of Miocene the continental deposits of Chota Group were involved in cylindrical folds characterized by a WNW–ESE direction of shortening; (b) a second compressive pulse occurred during Pliocene or early Pleistocene when lava flows dated 6 Ma were affected by NNE trending right-lateral strike–slip faults and fluvial deposits of 1.7 Ma were involved in N–S trending folds; (c) lacustrine, fluvial and volcanic intermontane deposits dating up to the middle Pleistocene were deformed during late Pleistocene by a system of strike–slip and reverse faults, consistent with a N–S direction of the greatest principal stress ($\sigma 1$), and by en-échelon folds with an average E–W axis, oblique to the NNE trend of the Cordilleras; (d) a last tectonic pulse involved also volcano-sedimentary deposits dating up to the Holocene, which were affected by an en-échelon NNE left-lateral normal and N–S pure normal faults responding to an E–W least principal stress ($\sigma 3$). The en-échelon arrangement of the post-Miocene structures, the predominance of strike–slip and oblique–slip motions and the presence of strike–slip faulting in the Cordilleras, lead us to interpret the Plio-Quaternary tectonic events in the frame of transpressive and transtensive deformation regimes. This evolution of the deformation styles is thought to be the result of the reactivation of the early Tertiary suture zone, laying beneath the volcano-sedimentary filling of the IV, by the differential motions between the Cordillera Occidental and Cordillera Real crustal blocks during Plio-Quaternary times.

1. IS THE INTERANDEAN VALLEY A GRABEN?

Topographic depressions associated with normal faulting are usually referred to as grabens. This association subtly implies an extensional genesis and a symmetric geometry of the whole structure. When such kind of deformations is found in a dominantly compressional environment, such as in the Andes, geologists are forced to find new explanations. This is the case of the compensated high topography model (Cross and Pilger, 1982) which has been applied successfully in the Peruvian Andes (Sebrier *et al.*, 1985) where normal faulting developed in the highest areas following an horizontal least principal stress (σHmin) perpendicular to the E–W convergence direction between Nazca and South America plates. The model considers the effect of the elevated mass of the High Andes

(body forces) as prevailing over the plate tectonic forces (boundary forces), so that the σ1 becomes vertical while the horizontal maximum stress (σHmax) constitutes the intermediate one (σ2). Another interesting model is the "Piggyback basin", which was introduced by Ori and Friend (1984) to describe all sedimentary basins that formed on active thrust sheets. The formation of this sort of basin occurs when new thrust-sheet ridges form in front of the previously active thrust margins. Sediments accumulation in piggyback basins is not related to subsidence or graben-type deformations but to the erosion of uplifting ridges of the internal piggyback thrust and external thrust sheets. In the Ecuadorian Andes normal

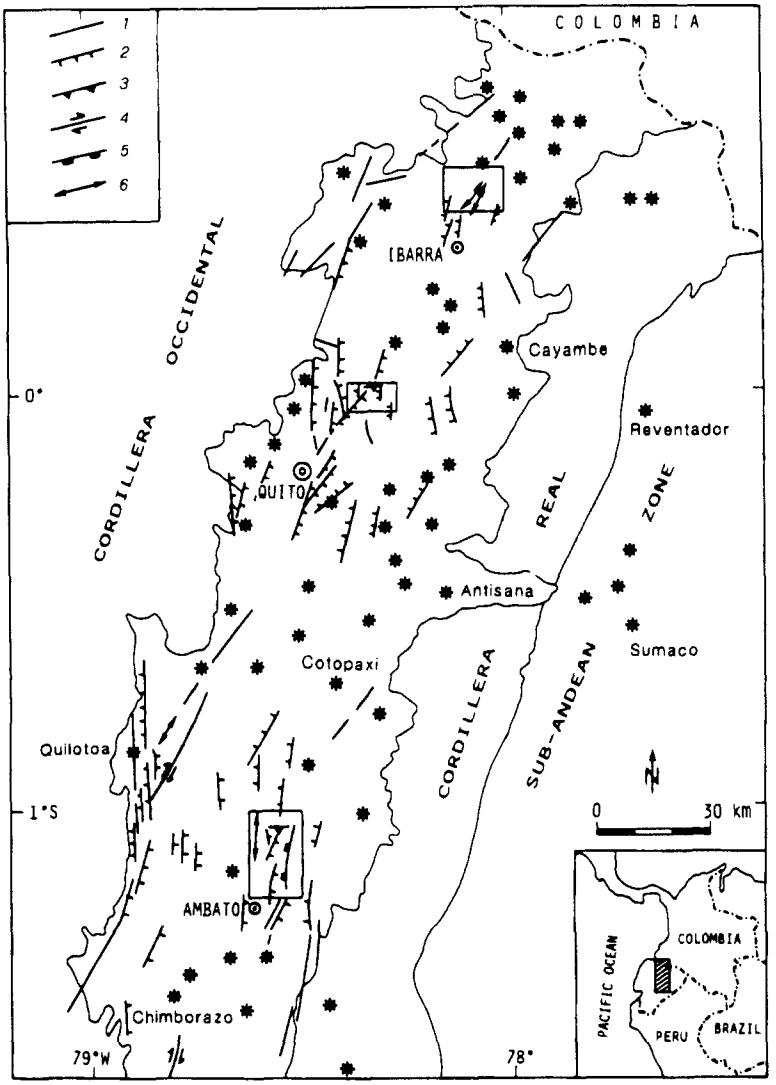

Fig. 1. Main faults and volcanic centres (*) of the studied part of the IV. 1, Fault with undetected motion; 2, normal fault; 3, reverse fault; 4, strike-slip fault; 5, flexure; 6, fold. Boxes represent location of Figs 2, 6 and 11. Inset shows the figure location.

faulting is confined to a unique main depression, elongated in a NNE–SSW direction which extends from the latitude 2°S to the Colombia border (Fig. 1). This depression is known as the Interandean Valley (IV), a descriptive term indicating its parallelism and its location between the two main mountain ranges of Cordillera Occidental (CO) and Cordillera Real (CR). A brief description of the structures intersecting the IV deposits was given in Hall *et al.* (1980), Baldock (1982, 1985) and Hall and Wood (1985). According to these studies the main faults belong to two sets trending NNE–SSW and NW–SE while the IV is a graben structure. However, Tibaldi and Coltelli (1989) found compressional deformation and N–S pure normal and NNE–SSW left-lateral normal faults affecting volcanic and sedimentary deposits of the IV that range in age up to the Quaternary. These faults show an asymmetric development in both strike and amount of displacement. These data suggest a more complicated structure, and make it difficult to apply in any simple way the compensated high topography model for the Ecuadorian Andes.

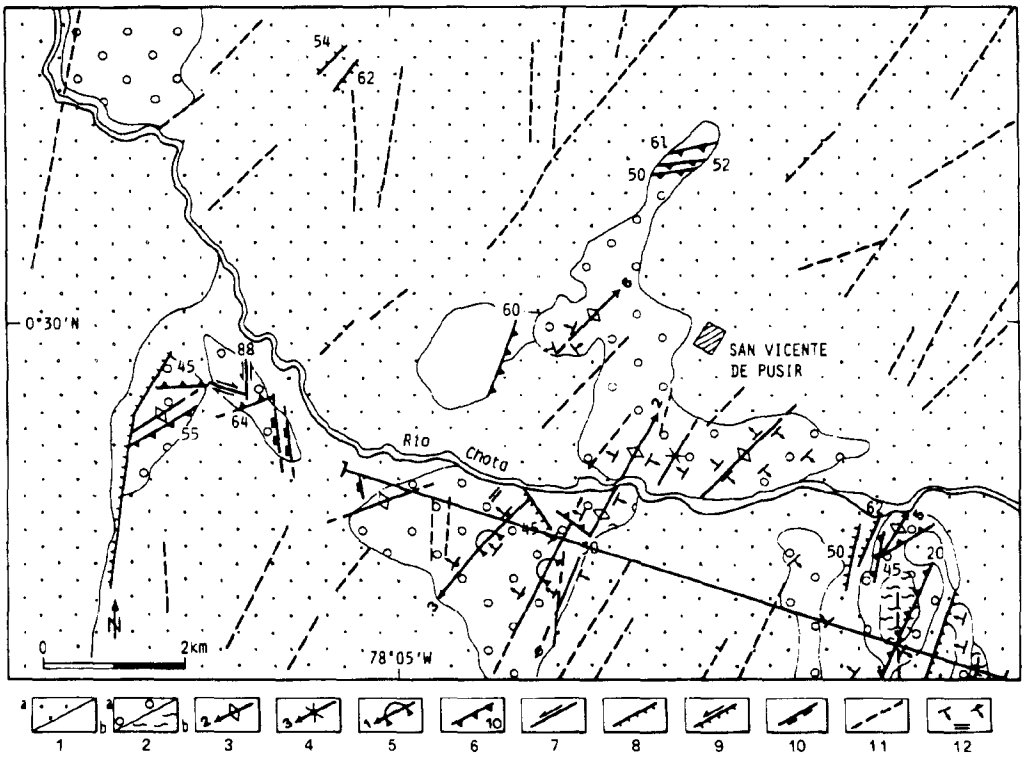

Fig. 2. Structural map of a representative area of the northern sector of the IV (from an unpublished structural map at 1:50,000 scale). See Fig. 1 for location. 1, (a) Latest Pleistocene–Holocene deposits unfaulted or affected by normal faulting, (b) Pliocene–middle Pleistocene rocks affected also by compressional deformations of the transpressional phases with a N–S or an E–W axis of shortening; 2, (a) Miocene rocks affected also by compressional deformation with a WNW–ESE axis of shortening, (b) metamorphic rocks of Paleozoic age; 3, anticlinal axis (with plunge); 4, synclinal axis; 5, axis of recumbent fold; 6, reverse fault with dip; 7, strike–slip fault; 8, pure normal fault; 9, oblique normal fault; 10, flexure; 11, photogeological lineament; 12, dip of strata: 1–75°, 76–90°, reverse. The WNW line is the section trace of Fig. 5.

In this paper we present structural field data collected in the volcanoclastic deposits of the IV and we then try to reconstruct its kinematic evolution. Our study leads to interpret the IV as a piggyback basin which first underwent a semi- continuous compressional regime, and then, during Quaternary times, experienced a transition from a transpressional to transtensional structural style.

2. ANALYSIS AND INTERPRETATION OF NEOGENE TO QUATERNARY STRUCTURES

Structural data presented in this chapter are derived from field surveys carried out in the last three years. They deal with macro- and mesoscale field observations that are integrated with some interpretations drawn from stereophotos at 1:50,000 scale. Macrostructures were used for the compilation of an unpublished 1:50,000 scale structural map, some examples of which are reported in Figs 2, 6 and 11. Separation of the various tectonic phases has been made possible by the direct field observations of fault crosscutting relationships or inferred from the stratigraphic position of the lithostratigraphic units involved in the deformations. K–Ar datings, paleontological age determination and stratigraphic studies, partially published in Barberi *et al.* (1988) and Coltelli and Tibaldi (1992), were used for the purpose of establishing the timing of tectonic phases. Fault kinematics is based on the analysis of striations and other tectoglyphs on the movement planes.

In the IV the largest structures are N–S en-echelon normal faults dipping mainly toward the East which dominate the western side of the depression (Fig. 1). On the eastern side NNE–SSW normal faults prevail and gradually disappear toward the CR. Several Quaternary stratovolcanoes and related pyroclastic products locally bury the tectonic structures. Where older continental sediments outcrop, they are affected by large folds with a length of hinge line ranging up to several kilometers.

An illustration of these structures is given in the following paragraphs through three representative examples in the northern, central and southern IV.

2.1. Northern sector

The best stratigraphic record of this area is exposed along the Chota Valley (Fig. 2). Here, the youngest rocks outcropping are fluvian conglomerates and pyroclastic deposits of late Pleistocene–Holocene age (DGGM, 1980a; Villalba, 1981; Coltelli and Tibaldi, 1992). N–S pure normal (pitch = 80–90°) and NNE–SSW left-lateral normal (pitch = 50–75°) faults dipping mainly to the west affect these units [Figs 2 and 3(a)]. On the western side of this area, N–S faults control the morphology of the most depressed part of the IV. Locally WNW–ESE transfer faults with oblique motions connect segments of the main normal faults. The oldest rock units in this sector are Pleistocene lacustrine and volcano-sedimentary deposits (Villalba, 1981), Pliocene andesite (Barberi *et al.*, 1988; Coltelli and Tibaldi, 1992) and Miocene continental deposits named Chota Group (Bristow

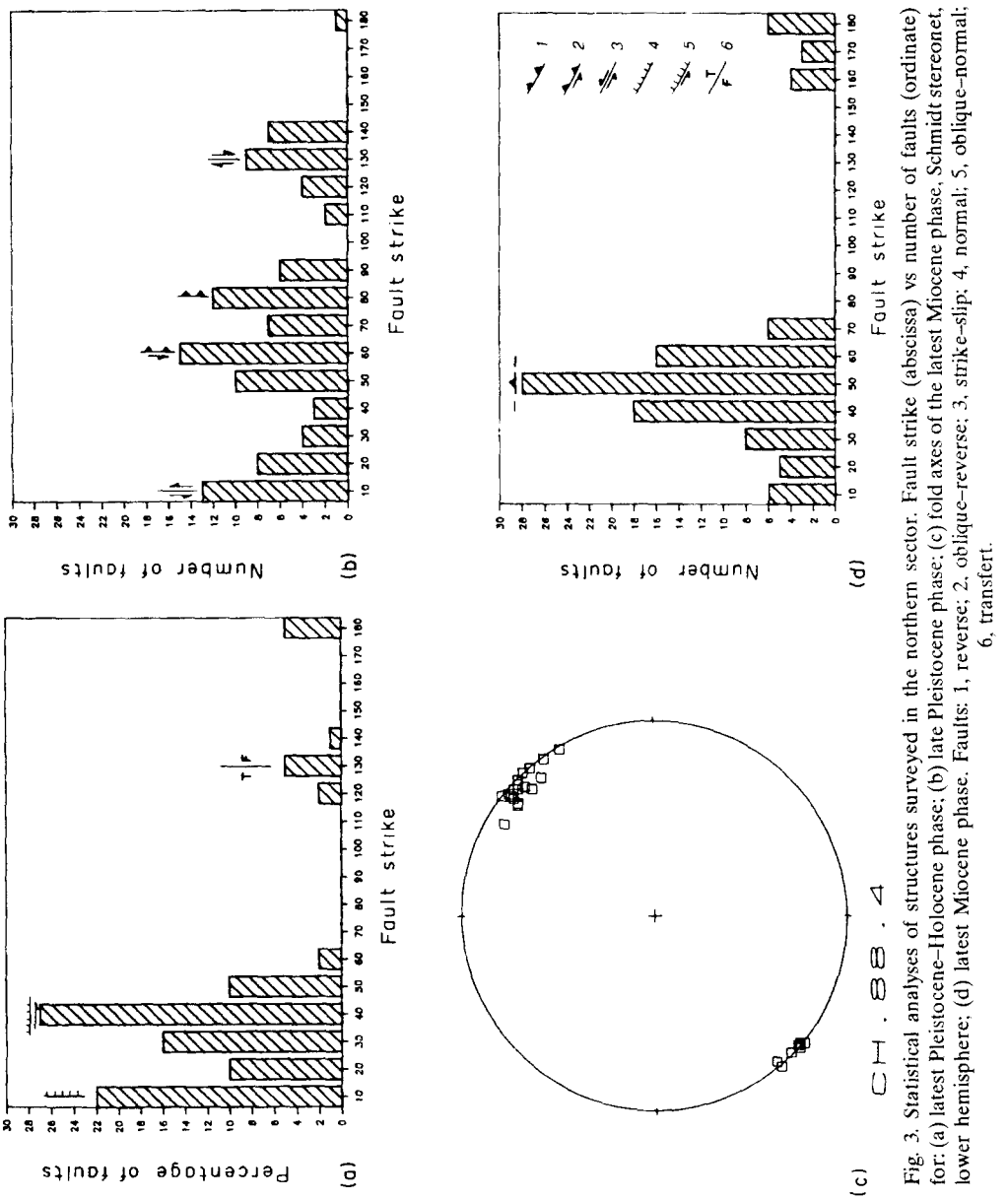

Fig. 3. Statistical analyses of structures surveyed in the northern sector. Fault strike (abscissa) vs number of faults (ordinate) for: (a) latest Pleistocene–Holocene phase; (b) late Pleistocene phase; (c) fold axes of the latest Miocene phase, Schmidt stereonet, lower hemisphere; (d) latest Miocene phase. Faults: 1, reverse; 2, oblique–reverse; 3, strike–slip; 4, normal; 5, oblique–normal; 6, transfert.

and Hoffstetter, 1977). These are also affected by compressional structures which are dislocated by the extensional faults systems.

Compressional deformations include folds and faults of various length and orientation. NW–SE right-lateral and NNS–SSW left-lateral strike–slip (pitch=5–20°) faults coexist with E–W reverse (pitch=75–90°) and NE–SW left-lateral reverse (pitch=40–72°) faults [Figs 2, 3(b), 4 and 5] dipping at high angle and with small displacement. This system affects all the rock units up to the Pleistocene. Although the Pleistocene age is quite uncertain, due to the classification of a mammalian (Villalba, 1981), the compressional fault system was recognized in andesitic rocks dated as 3.46 Ma using the K–Ar method (Barberi *et al.*, 1988). In the Chota Group deposits these fault systems dislocate structures inherited from an older compressional phase. In fact sandstones and conglomerates of Chota Group were involved in cylindrical east-vergent folds with 1–2 km-long-hinge lines (Figs 2 and 5) trending NNE–SSW in average [Fig. 3(c)]. In the same units NNE–SSW trending pure reverse faults (pitch=79–90°) are also widespread [Fig. 3(d)]. These faults, ranging in dimension from some metres to tens of metres, dip at low angle and show large displacement.

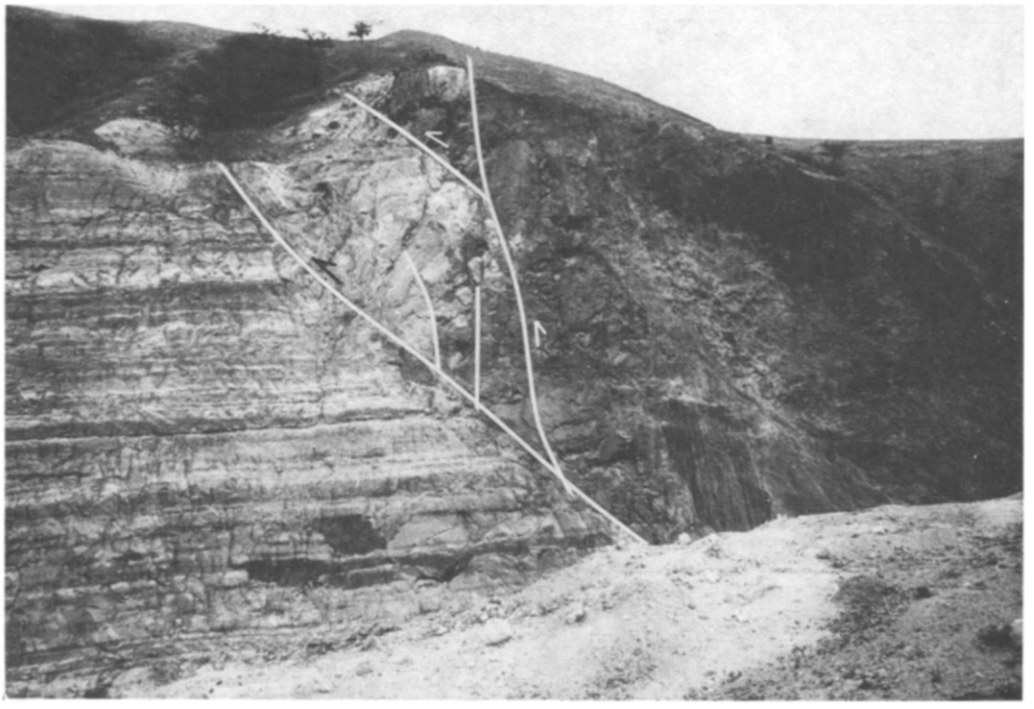

Fig. 4. Northern side of Chota Valley. Highly tectonized lava (on the right side of the picture) in contact with Pleistocene lacustrine deposits along a NE transpressional fault system. Motion has been obtained through the analysis of the tectoglyphes on the fault planes. Outcrop view width is about 40 m and is toward NE.

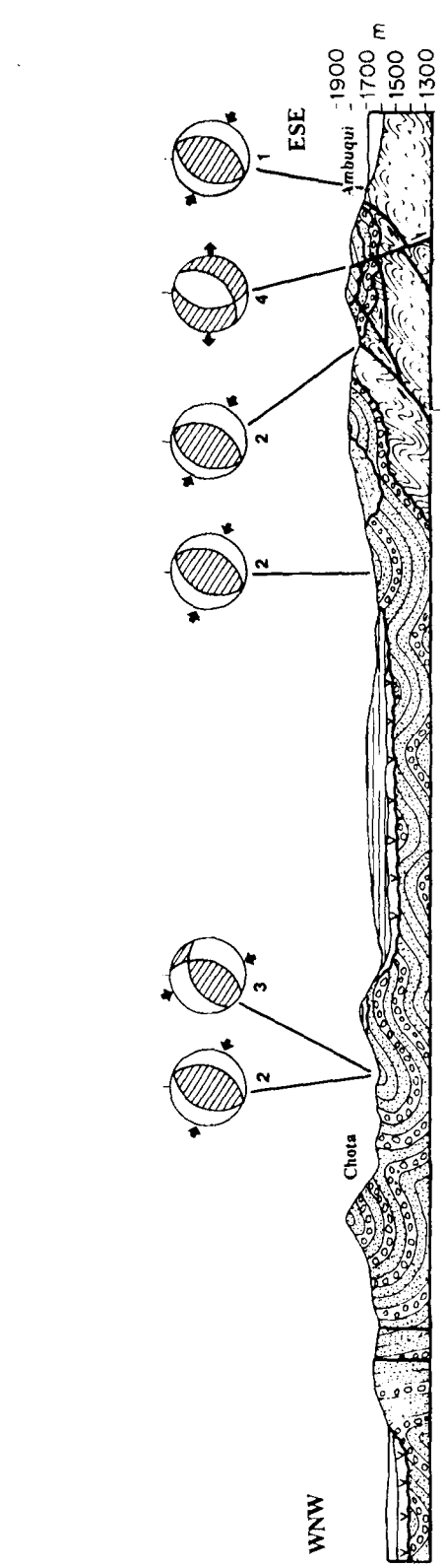

Fig. 5. Geological cross-section along the Chota Valley. Section trace in Fig. 2. 1, Recent alluvial deposits; 2, colluvium deposits; 3, Holocene pyroclastic rocks; 4, faulted recent conglomerates affected by extensional tectonics; 5, sedimentary rocks of the Chota Group (Miocene); 6, metamorphic rocks of the Ambuqui Formation (Paleozoic); 7, faults; 8, angular unconformity. Mean direction of compression and extension deduced by fault plane are represented on Schmidt stereonet as: 1, Pre-latest Miocene phase; 2, latest Miocene phase; 3, late Pleistocene phase; 4, latest Pleistocene–Holocene phase; the three sites closer to the village of Chota resume data collected on faults lying at a short distance from the section.

To summarize, the following deformation phases can be recognized in the northern sector of the IV:

(a) a compressional phase of Pliocene age which produced NNE–SSW cylindrical folds and low angle pure revers faults;
(b) a not well time-constrained Pleistocene phase yielding high angle strike-slip, pure reverse and oblique faults kinematically compatible with a N–S compression;
(c) an Holocene extensional phase with the development of N–S pure normal and NNE–SSW left-lateral normal faults.

2.2. *Central sector*

Guayllabamba depression. In the Guayllabamba depression (Fig. 6), which is the most suitable study zone of the central sector, outcropping rock units range in age from early Pleistocene to Holocene (DGGM, 1982). N–S pure normal

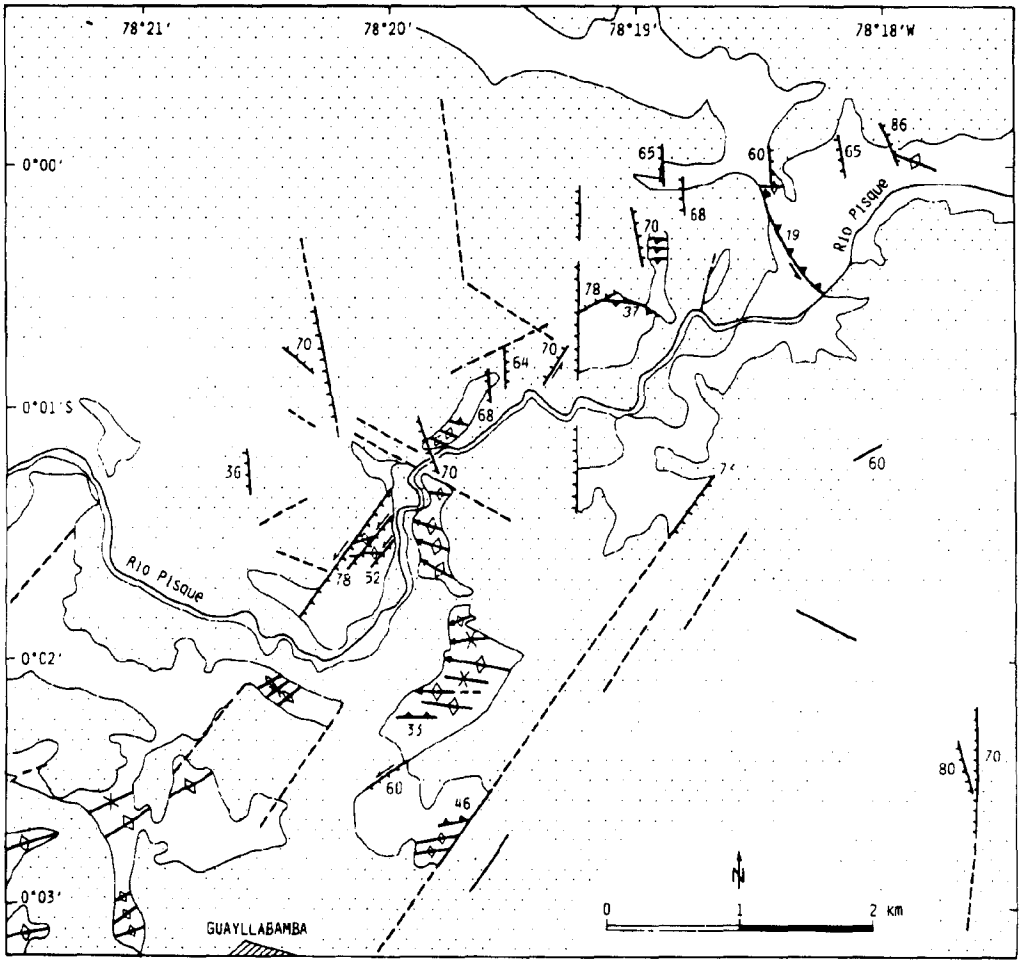

Fig. 6. Structural map of a representative area of the central sector of the IV. Legend as in Fig. 2.

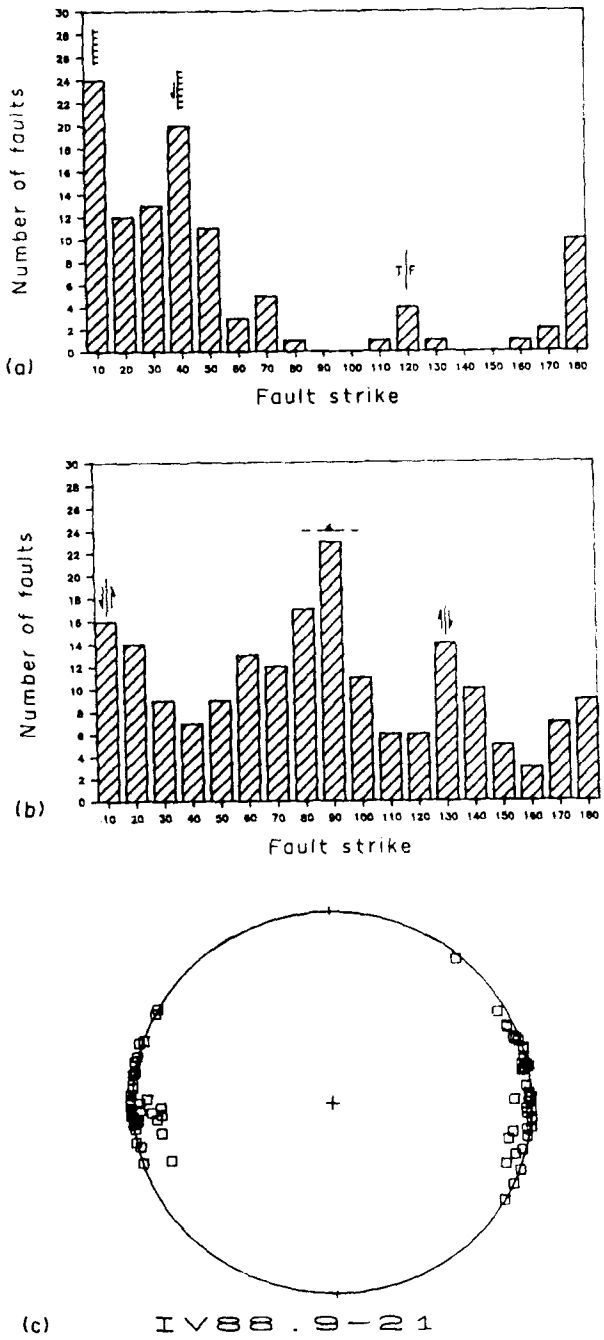

Fig. 7. Statistical analysis of structures surveyed in the central sector. Fault strike (abscissa) vs number of faults (ordinate) for: (a) latest Pleistocene–Holocene phase; (b) late Pleistocene phase; (c) fold axes of the late Pleistocene phase, Schmidt stereonet, lower hemisphere.

and NNE–SSE left-lateral normal faults affect the volcano- sedimentary succession up to the deposits of the second plinian eruption of the Mojanda volcano (Coltelli and Tibaldi, 1992) [Figs 6 and 7(a)]. On the basis of tephrostratigraphic studies this eruption occurred at the end of the Pleistocene or at the beginning of the Holocene. Continuation of this extensional tectonic phase during Holocene is confirmed by systematic N–S extensional fissures 2–10 cm-wide filled by Holocene colluvium which are visible in a quarry 1 km west of Guayllabamba.

Discrimination between gravitational and tectonic structures in the Guayllabamba depression. While in the northern sector of the IV the Plio-Quaternary times were characterized by the deposition of conglomerates and lavas, in the Guayllabamba area sedimentation consisted essentially in accumulation of ashes, pumices and diatomites in a lacustrine environment. In this sector, the older rock units of early-middle Pleistocene age are involved in several folds of various amplitude and hinge line length. The presence of soft, highly incompetent, water-saturated sediments created the rheological conditions of the development of several folds with small wavelength. In addition, observable deformations occurred within the most surficial strata with negligible lithostatic pressure.

Azimuths of axes of largest folds invariably range between ENE and ESE [Figs 6 and 7(c)]. Most of the folds are of non-cylindical type and do not show

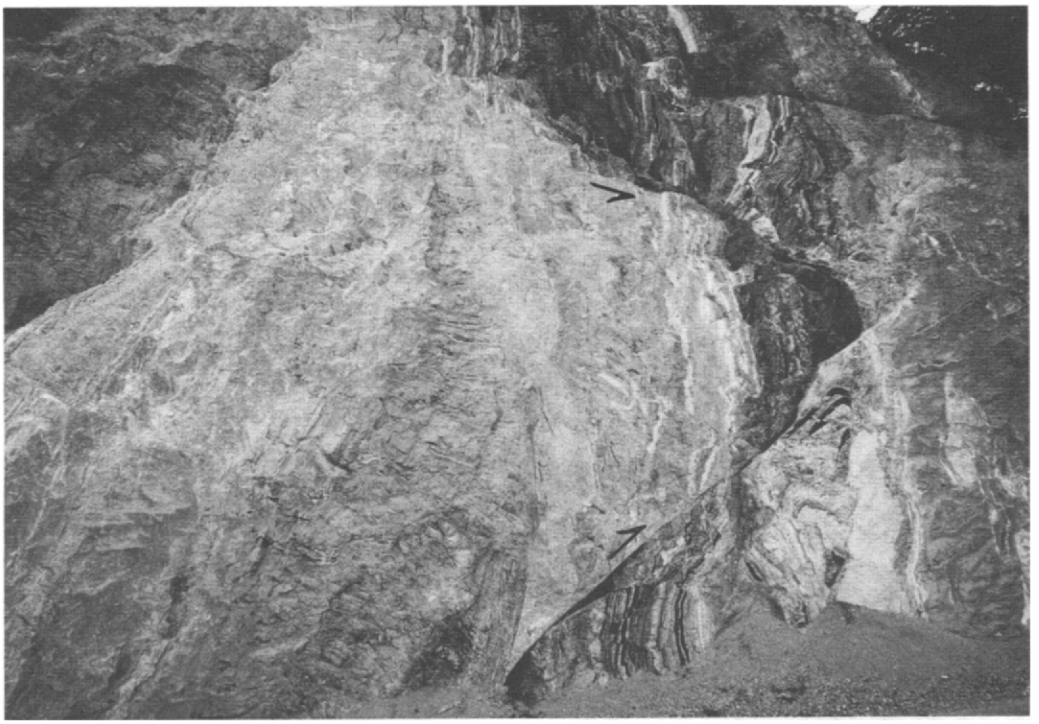

Fig. 8. North-central sector of the Guayallabamba depression; early-middle Pleistocene volcano-sedimentary deposits involved in a compressional tectonic wedge. NNW is on the right side of the photo. View width is about 15 m.

a constant vergence. Small scale chaotic folds are also locally present. They show amplitudes ranging from decameters to meters and have various orientations of their fold axes. They could probably be interpreted as gravitational decollement deformations or as readjustments between major structures. In this study we considered that compressional deformations were induced by regional tectonics, and not by gravity, when they display the following features:

- folds axes relatively parallel;
- planar fold axial planes;
- large amplitude;
- competent non-plastic units, as cemented conglomerates, involved in folding;
- absence of interstratum slip structures;
- existence of widespread systematic and large strike–slip and reverse faults.

In addition it should be noted that:

(a) everywhere normal faults dislocate compressional structures of brittle and plastic type;

(b) compressive deformations developed within units older than the latest Pleistocene Cangahua Formation;

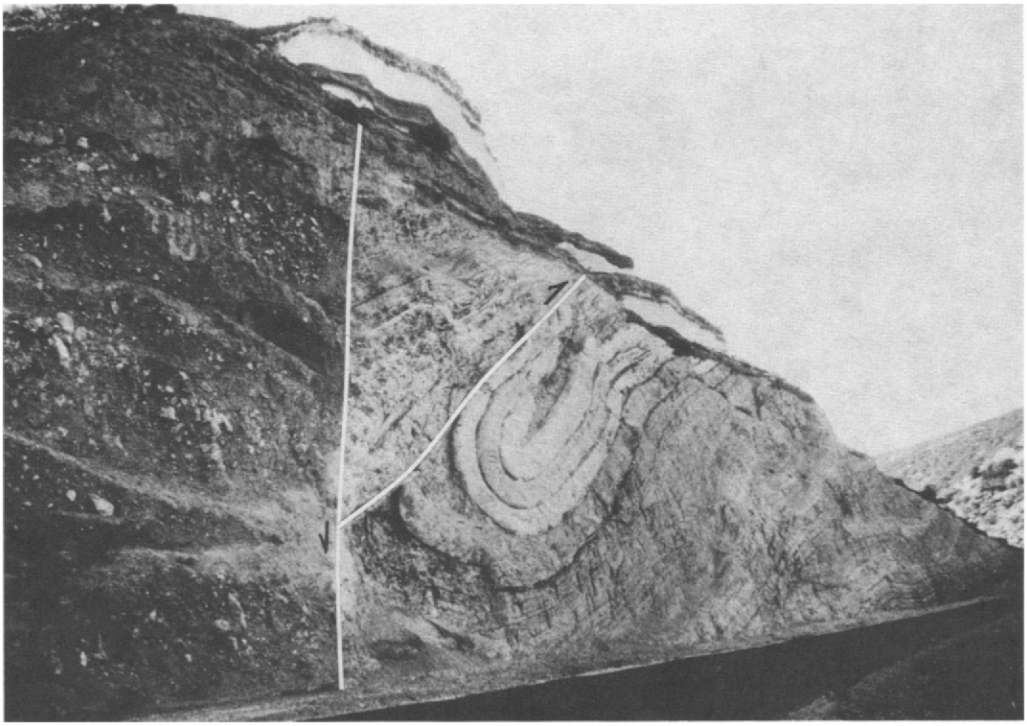

Fig. 9. Stretch of the Guayllabamba–Otavalo highway viewing westward. Road cut shows a latest Pleistocene or Holocene synsedimentary normal fault (on the left) and a late Pleistocene south dipping reverse fault. Compressional motion produced drag folding in the footwall. View width is about 70 m.

(c) fault strikes are more scattered than in the northern sector but converge in three main groups: NW–SE right-lateral and NNE–SSW left-lateral strike–slip faults and E–W reverse faults [Fig. 7(b)];
(d) fault spacing is very small, ranging from decimeters to tens of meters;
(e) attention was focused on the largest structures (Fig. 8); and
(f) neither large nor small faults show a radial patterns consistent with the gravitational collapse origin proposed by DGGM (1982) for the Guayllabamba depression.

DGGM (1982) geologic map, in fact, shows the compressional deformations recorded in the S. Miguel Desordenado Formation as the result of gravity sliding along normal faults limiting, with a circular perimeter, the Guayllabamba depression. This genesis would imply transport vergence toward the centre of this area along slip planes with strike sub-parallel to the circular faults. On the contrary, transport vergence and fault strike are often opposite to the ones expected from the gravitational model, as, for example, along the road leaving northwards the town of Guayllabamba. Road cuts show large E–W reverse faults dipping to the south with clear indicators of northward transport as slickenside lineations and drag folds (e.g. in Fig. 9), while the position in proximity of the northern limit of the Guayllabamba depression would suggest southward motion. Another example in the same area is a large ramp and flat structure given by an obsidian

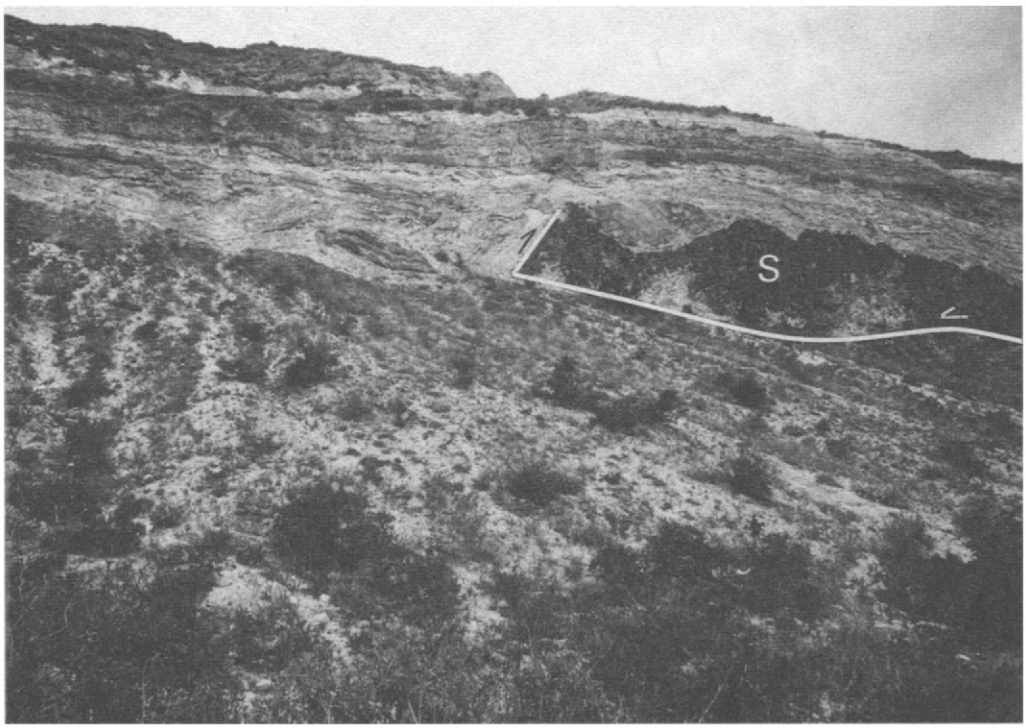

Fig. 10. Northern part of the Guayllabamba depression. Front of an obsidian thrust sheet (S) pushed northward along a ramp and flat structure. Sedimentary deposits in front of the sheet are deformed in a ductile fashion. View width is about 200 m and is eastward.

sheet pushed northwards along south dipping slip planes (e.g. in Fig. 10); sandy deposits form the footwall while finer silty sediments were pushed and highly folded in front of the ramping obsidian sheet. At a closer look, fold axes are parallel and coherent with the geometry of the frontal hanging-wall block and the low wavelength of the folds is compatible with the high difference of rheology between fine lacustrine deposits and obsidian lavas. Finally, it is also worth pointing out that close to the eastern or western limits of the Guayllabamba depression the fold axes do not parallel the N–S strike of the hypothesized detachment surfaces.

Quito area. Normal deformations (pitch=56–90°) were recognized also in a wide zone around the town of Quito. Faults have displacements of centimeters to meters and strike from NNW to NNE. Rocks involved in the deformation date up to the Holocene. The city of Quito is built on a succession of Quaternary lava flows and pyroclastic rocks which systematically dip toward the west and are affected by small normal faults. These rocks are limited to the east by two large eastward dipping scarps (scarp altitude of 100–200 m) and we interpret the whole structure as a tilted block bounded by normal faults. In addition, on the western side of the Cordillera Real, near the Quito-Baeza road, NNE–SSW striking gash fractures 5–19 cm-wide affect moraine deposits belonging to the last glaciation.

Along the Guayllabamba River 16 km NNE of Quito, the easternmost front of the Cordillera Occidental terranes outcrops at the base of a deep canyon. Here volcanic rocks of the Macuchi Formation are faulted in wedge structures dipping to the WNW. Within one of these wedges an E–W fold affects lacustrine sediments very similar to the Quaternary ones of the central sector of the IV. The lacustrine sediments are tectonically overridden by lavas of the Macuchi Formation, thus indicating a Quaternary reactivation of the front of the CO.

In conclusion, the central sector of the IV was affected by:

(a) a late Pleistocene compressional pulse which produced E–W folds and reverse faults, NW–SE right-lateral and NNE–SSW left-lateral strike–slip faults;

(b) a latest Pleistocene to Holocene extensional pulse characterized by the development of N–S pure normal and NEE–SSW left-lateral normal faults.

2.3. *Southern sector*

This sector was mainly studied in the Latacunga and Ambato basins. In these areas the youngest deformations are also represented by N–S en-echelon pure normal faults (pitch=80°) especially developed along the western side of the IV (Fig. 1) and NNE–SSW left-lateral normal faults (pitch=59–80°) dominating mostly in the eastern part [Figs 11 and 12(a)]. This fault system affects the volcano-sedimentary succession up to the Holocene units, according to the age proposed by DGGM (1978).

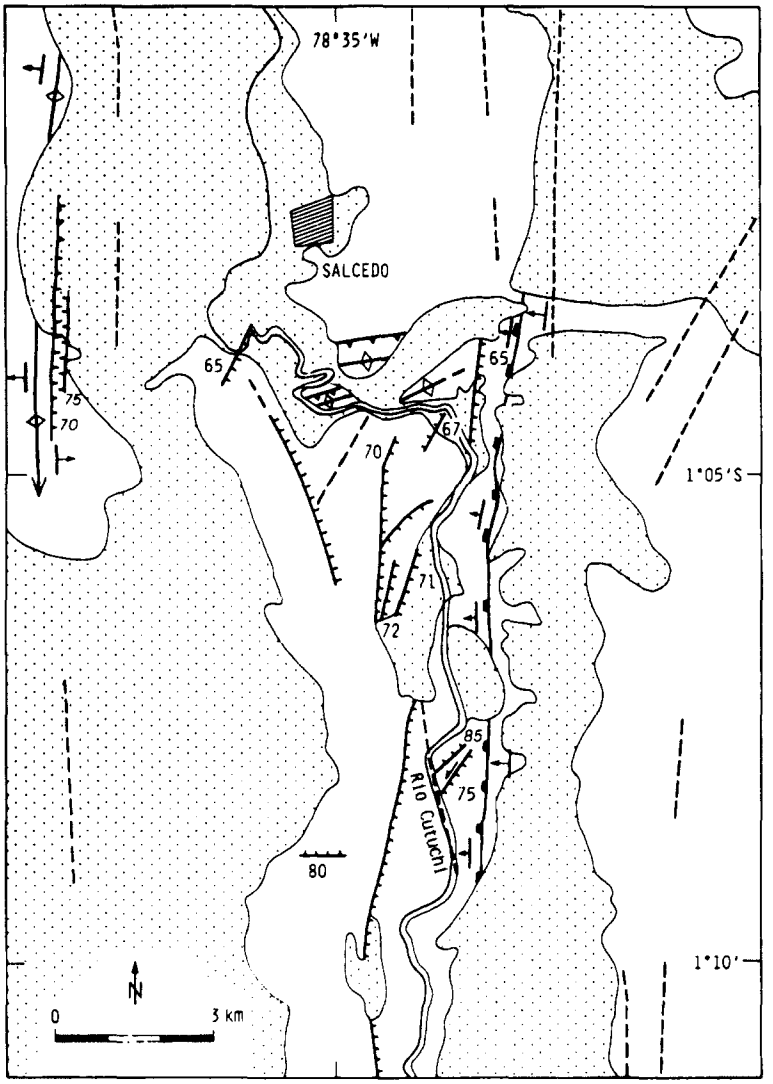

Fig. 11. Structural map of a representative area of the southern sector of the IV. Legend as in Fig. 2.

The E–W folds and reverse faults were developed within fluvio-lacustrine and pyroclastic rocks of probable Pleistocene age [Figs 12(b) and (c)]. Folds are similar in dimension to the largest ones of the central sector, ranging from tens to hundreds of meters of hinge line length. By contrast, two large N–S folds affect fluvial conglomerate with interlayered lava flows which were dated at 1.7 and 1.8 Ma (Bonhomme *et al.*, 1990). The largest fold lies few kilometers to the west of Latacunga and has an 8-km long hinge line. About 3 km to the east of Latacunga the same rocks are deformed into a N–S flexure outcropping for nearly 11 km. These fluvial deposits, known as the Latacunga Formation, testify a large increase of the erosion rate at both margins of the IV which could be related to tectonic motions. The structural depression created in the middle of

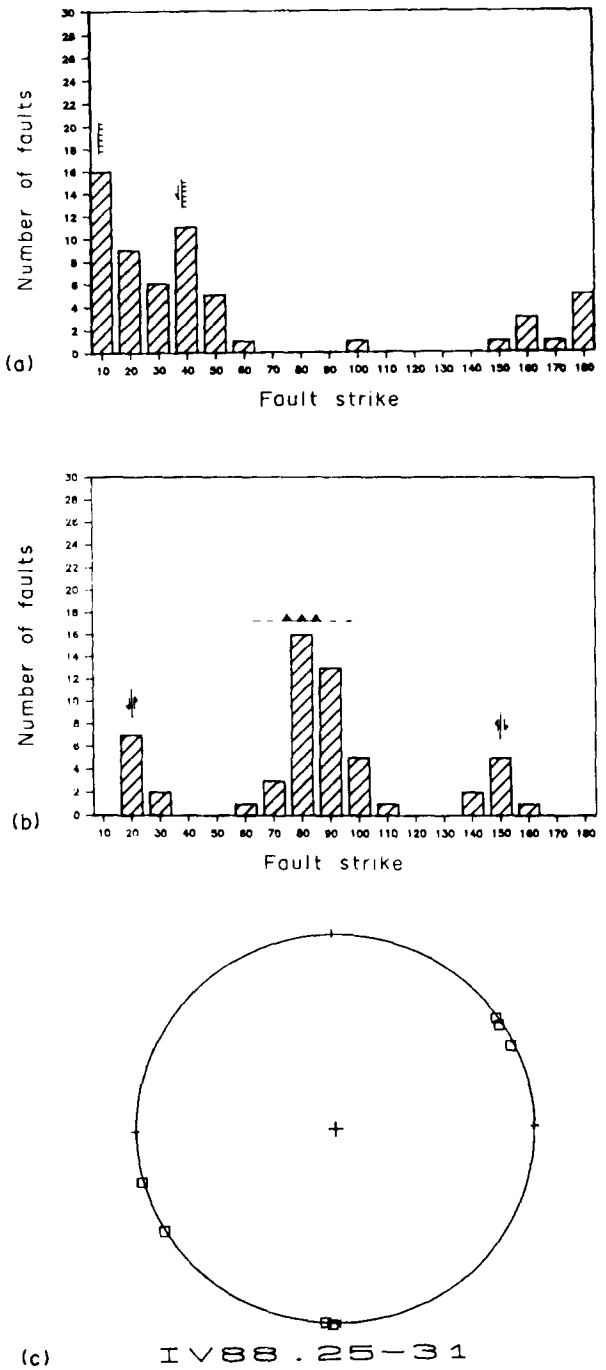

Fig. 12. Statistical analysis of structures surveyed in the southern sector. Fault strike (abscissa) vs number of faults (ordinate) for: (a) latest Pleistocene–Holocene phase; (b) late Pleistocene phase; (c) fold axes of the late Pleistocene (E–W) and early Pliocene (N–S) phase, Schmidt stereonet, lower hemisphere.

the parallel anticline and flexure is filled by a pumice flow related to the Holocene Chalupa caldera (M. Coltelli, personal communication).

Some tens of kilometers to the west, near the Quilotoa volcano we recognized a large NNE right-lateral strike–slip fault (Fig. 1). The fault is some tens of kilometers long and dislocates lava flows dated as 6.1 Ma (Barberi *et al.*, 1988). It is covered by unfaulted pyroclastic flows of Holocene age.

Finally, to the southwest of the area represented in Fig. 11, rocks belonging to the Miocene Moraspamba Formation (DGGM, 1980b) are involved in a cylindrical fold with a NE–SW 2 km-long hinge (shown in Fig. 1).

In summary, the volcanic and sedimentary units of the southern sector of the IV were deformed during three main phases:

(a) a latest Miocene compressional phase which created NE–SW folds;
(b) a Pliocene or/and early Pleistocene compressional pulse which produced large NEE right-lateral strike–slip faults and N–S folds and flexures;
(c) a middle or late Pleistocene compressional pulse which produced E–W folds and reverse faults;
(d) a latest Pleistocene to Holocene extensional pulse responsible for the N–S normal and NNE–SSW left-lateral normal faults.

3. QUATERNARY STRESS REGIMES

Fault slip data were used to compute orientations of principal stresses through a computer method based on Carey's algorithm (Carey, 1979). Data from tilted faulted blocks were not considered, or were first restored to their original positions. Each solution is based on a minimum of 6 striated planes and was accepted if at least in 80% of them the deviation angle between observed and predicted stria was $<15°$. Faults belonging to the latest Miocene and Pliocene compressional events were not processed because of the uncertainty of the tensor orientation due to the possible rotations induced by the younger phases.

From the comparison of the structural evolution in the different sectors of the IV, it can be deduced that the youngest compressional deformations developed during middle and late Pleistocene. Strike–slip and reverse faults are compatible with an average N–S direction of the greatest principal stress ($\sigma1$) laying within a horizontal plane (Fig. 13). At the sites where transcurrent faulting was dominant, $\sigma3$ was horizontal and oriented E–W, while reverse faulting prevailed where the $\sigma3$ interchanged with the $\sigma2$. It is worth noting that the $\sigma1$ orientation was oblique to the NNE–SSW orientation of the Cordilleran structures and that its direction was rather constant along all the IV.

Latest Pleistocene–Holocene normal faulting occurred in response to a horizontal $\sigma3$ with a mean E–W orientation (Fig. 14). Depending upon the other horizontal principal stress, which was either $\sigma2$ or $\sigma1$, normal and left-lateral normal faulting or normal left-lateral, respectively, developed. Also in this period the orientation of $\sigma3$ was quite constant along the IV. This supports a homogeneous behaviour and a similar deformation history for the entire basin.

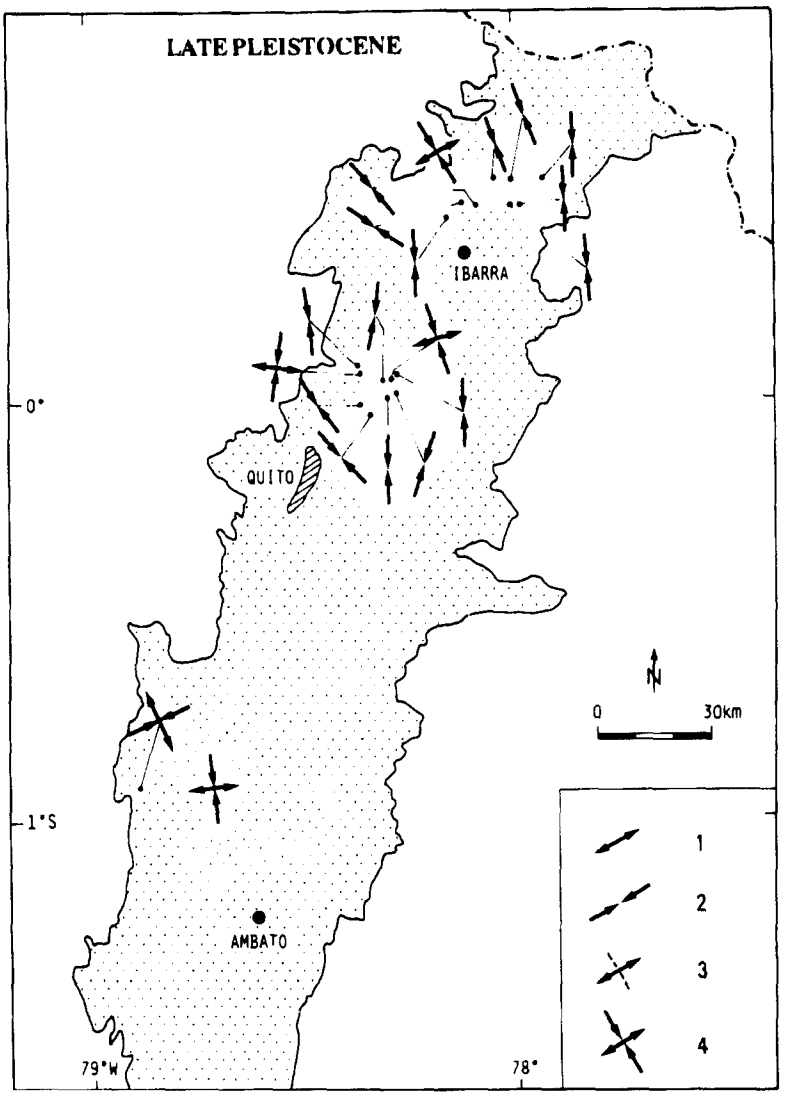

Fig. 13. Late Pleistocene stress regime. Converging and diverging arrows represent direction of greatest ($\sigma 1$) and least ($\sigma 3$) principal stress computed with a program based on Carey's algorithm (1979). Deformation mechanism is given by: 1, normal faulting; 2, reverse faulting; 3, oblique extension; 4, strike-slip faulting.

4. TECTONIC EVOLUTION OF THE SURROUNDING AREAS

The CO is mainly formed by Cretaceous volcanic rocks with island arc affinity (Macuchi Fm.) (Henderson, 1979; Lebras *et al.*, 1987) covered by discontinuous flysch-like deposits of Cretaceous to Eocene age. It is considered an "exotic terrain" accreted onto the South American margin during a major tectonic phase in Early Tertiary time (Feininger and Bristow, 1980; Lebras *et al.*, 1987; Roperch *et al.*, 1987) while during Neogene–Quaternary times was affected only by minor tectonic activity (Pasquarè *et al.*, 1990; Ferrari and Tibaldi, 1992).

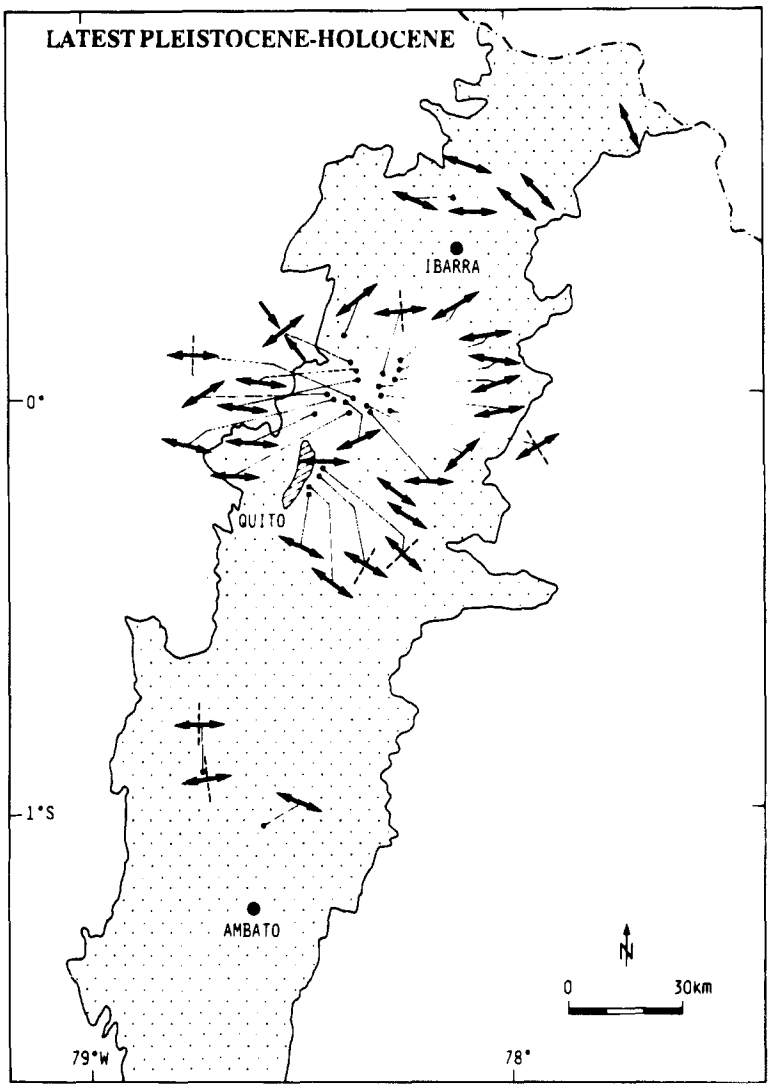

Fig. 14. Latest Pleistocene–Holocene stress regime. Legend as in Fig. 13.

In this framework, the IV lies above the suture between the CO island arc and the continental paleomargin represented by the CR.

The CR is part of a metamorphic belt that runs continuously from the Colombia to the Peruvian border. The CR is made by distinct metamorphic associations dating back to Precambrian and Paleozoic (Baldock, 1982) and has undergone several orogenic phases since the Cretaceous and probably since Paleozoic times (Zeil, 1979). The Andean orogenesis, due to the accretion of old Pacific plates and subduction of the Nazca Plate under the South American Plate, produced an overlap of the CR units eastwards onto the Sub-Andean zone along several WNW dipping thrust planes with a climax during the Miocene (Baldock, 1982). This phase was followed by Pliocene right-lateral thrusting along NNE striking

planes (Pasquarè *et al.*, 1990). The Quaternary tectonics is characterized by the coexistence of strike–slip and thrust deformation. Motion takes place along major NNE–SSW trending right-lateral strike–slip faults, some N–S en-echelon thrust and oblique-thrust faults and some rare secondary NW–SE trending left-lateral strike–slip faults (Ferrari and Tibaldi, 1992).

5. DISCUSSION

5.1. A model for the genesis and the evolution of the IV

As explained in the previous paragraph, four main tectonic pulses deformed the rock units of the IV during the end of Miocene and the Holocene. Deformation alternated, or accompanied, the accumulation and filling of the IV by fluvial, lacustrine, glacial and volcanic deposits. If we assume that continental basin sedimentation and volcanism reflect subsidence and extensional tectonics (i.e. genesis and development of IV as a graben structure), we should invoke several inversion of the tectonic regime to explain this alternation of extensional and compressional phases. Such a succession of phases seems unlikely in the light of the short time span during which they should have taken place. In addition recent studies have shown that middle Miocene to Quaternary compressional deformations and uplift of the Ecuador forearc basins are related to a period of continuous high convergence rate (Daly, 1989). Therefore we propose a simpler explanation taking into account some observations and new data.

(a) First of all, the IV fill conceals a major suture between the oceanic terranes accreted during early Tertiary times and older terranes forming the South America

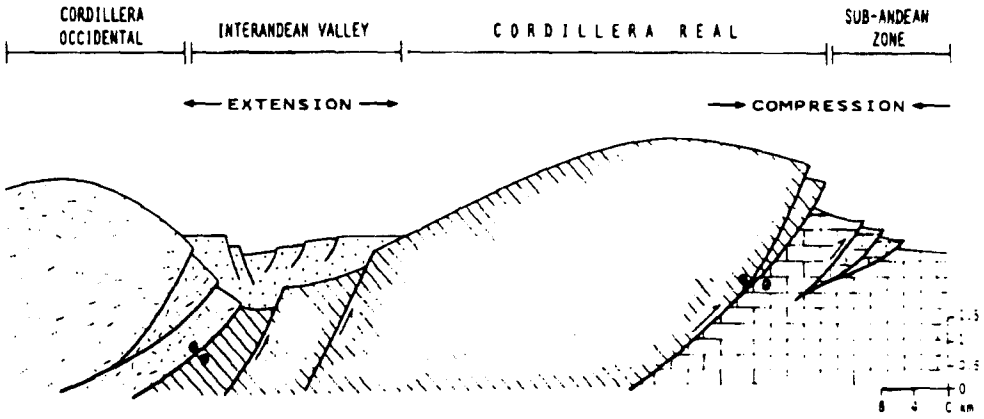

Fig. 15. Schematic WSW–ENE crustal section through the Ecuadorian Andes at Quito latitude. In this interpretation, based on surface geological and structural observations (Baldock, 1982, 1985; Pasquarè *et al.*, 1990; our unpublished data) and on geophysical data (Feininger, 1977; Feininger and Seguin, 1983), the IV is interpreted as an oblique piggyback basin carried on the more active CR transpressive sheet. Present deformations imply a relative divergence between the CR and the CO crustal blocks. A transcurrence component of motions is represented by arrows going outside and inside the page (encircled point and cross respectively). See text for details.

paleomargin (Feininger and Bristow, 1980; Lebras *et al.*, 1987; Litherland and Aspden, 1990). Mesozoic rocks of the Macuchi and Silante Formation were thrust during Oligocene onto the metamorphic Paleozoic Belt of the CR. Geophysical prospecting confirms that the suture lies under the deposits of the IV (Feininger and Seguin, 1983). The geometry of the suture zone fault system can be inferred by the thrust and reverse faults affecting the CO rocks units. Field inspections along several transects showed that these faults have a relatively constant NNE–SSW strike and WNW dip. Nevertheless, Juteau *et al.* (1977) recognized ophiolitic slices of the CO dipping steeply towards the East and interpreted this setting as resulting from accretion along east-dipping thrust planes. By contrast, in an E–W transect, across the CO at the latitude of 1°37'S along the valleys of Rio Pililag, Rio Ganquis and Rio Galera, we surveyed a dominance of east-vergent folds and west-dipping faults and strata. This geometry, also proposed in Baldock (1982, 1985), seems more coherent with the interpretation of the structures as due to obduction.

(b) The E–W fold affecting lacustrine sediments overthrust by rocks of the Macuchi formation we found in the central sector of the IV, is consistent with a Quaternary reactivation of the buried suture.

(c) The normal faults within the IV are concentrated in a belt running NNE–SSW along the middle-western part of the valley. Volcanics and volcano-sedimentary deposits to the east are relatively undeformed and overlap the back of the CR thrust complex, while to the west (*cf.* point b) the transition to the CO occurs through a relatively more deformed belt passing abruptly to the frontal zone of the western thrust complex (i.e. CO).

Bearing in mind these observations, we propose that the IV could be a basin carried piggyback (passively) on a thrust complex (Fig. 15). In our case the Miocene climax of compressional deformations in the external front of the CR thrust system (Baldock, 1982) represents the activation of a new thrust sheet of regional extension which, in turn, is coeval with the accumulation of the oldest clastic deposits outcropping in the IV (e.g. the Chota Group and Morraspamba Fm.). The IV filling needs no extensional tectonics but simply erosion of uplifting thrust belt and relative subsidence in a compressional environment, as already recognized in other similar structural settings (Pieri, 1983; Ori and Friend, 1984; Ori *et al.*, 1986; Cook and Clark, 1990). Reactivation of the internal thrust belt (CO) with a low rate of approaching to the external more active thrust belt (CR) could produce folding and compressional faulting of the piggyback filling. A high rate of volcanic activity occurred in coincidence with the blocking of the convergence between the two thrust belts (Barberi *et al.*, 1988). On the contrary, a low rate of moving apart of the CR with respect to the CO could produce extensional deformations in the deposits of the IV. This last mechanism contributed to the present architecture of the studied area, where N–S en- echelon pure normal faults to the west, NNE–SSW left-lateral normal faults to the east and a dominant westward tilting of blocks created a semi-graben structure with a roll-over anticline (Fig. 16).

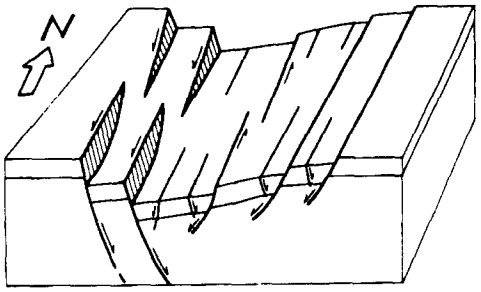

Fig. 16. Schematic block diagram showing the present geometry of the IV structure. En-echelon N–S pure normal and NNE–SSW left-lateral normal faults create dominant westward tilting of layering resulting in a semi-graben structure with a roll-over anticline.

5.2. Transpression and transtension

Important changes in the deformation mechanisms occurred between the first (end of Miocene) and the second (Pliocene–earliest Pleistocene) pulse, and between the latter and the following Quaternary pulses. Folds which developed during the Tertiary in the CO and CR have axes ranging between N–S to NE–SW (Baldock, 1982; Pasquarè *et al.*, 1990) with a maximum shortening axis directed WNW–ESE. The NNE–SSW trending cylindrical folds and pure reverse faults developed within the Miocene sediments of the IV are thus coherent with the regional deformations in the Cordilleras which are related to the latest Miocene WSW compression. The following Pliocene–earliest Pleistocene phase deformed the deposits of the IV creating N–S folds and flexures (usually the surficial

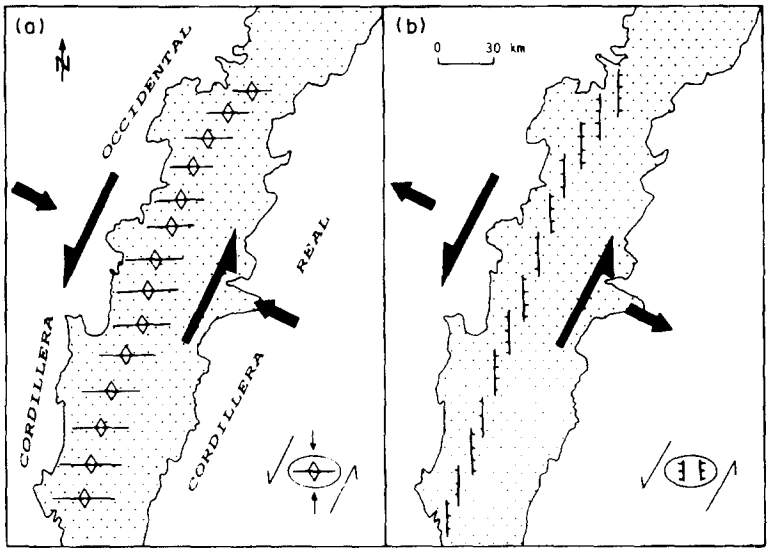

Fig. 17. Kinematic interpretative model of structures presented in this work. (a) Compressive deformations developed in response to a left-lateral transpressive pulse of late Pleistocene age; (b) normal faulting developed within a transtensive pulse of latest Pleistocene–Holocene age.

expression of blind thrusts) and NNE right-lateral strike–slip faults. These are compatible with a simple shear mechanism of deformation acting along a NNE right-lateral shear zone. The subsequent pulse created E–W non-cylindrical folds and reverse faults oblique to the Cordillera trend and several strike–slips faults. These deformations show an en-echelon arrangement along a NNE–SSW belt running in the central-western part of the IV. Finally, stress computation in many sites shows a N–S horizontal $\sigma 1$ and E–W horizontal $\sigma 3$ representing a transcurrent mechanism of deformation (Figs 13 and 14).

All the post-Miocene deformations observed along the IV can be explained by transcurrent kinematics. The N–S structures developed during the earliest Pleistocene are compatible with the NNE right-lateral strike–slip faults and could be interpreted as a surficial transpressive deformation induced by relative right-lateral transcurrent motions between CO and CR combined with a minor component of convergence. The following E–W compressional structures could be envisaged in an inversion of the sense of motion with left-lateral transpression [Fig. 17(a)]. This is in accordance with the eastward concentration of the right-lateral strike–slip motions (Ferrari and Tibaldi, 1989; Tibaldi, 1990; Pasquarè *et al.*, 1990). The cause of the post-Miocene transcurrence can be seen in the collision of the Carnegie Ridge with the Ecuadorian Trench dated from Daly (1989) at 8 Ma.

During the latest Pleistocene to Holocene en-echelon N–S pure normal and NNE–SSW left-lateral normal faults developed within an NNE–SSW elongated belt. Stress computation shows an orientation of the σHmax and the σHmin similar to the previous transpressive pulse, with a rotation of the tensor axes (horizontal $\sigma 3$ and $\sigma 2$). In the same period large NNE–SSW right-lateral strike–slip and reverse faults developed in the CR (Tibaldi, 1990; Tibaldi and Ferrari, 1990; Ferrari and Tibaldi, 1992). These data confirm the endurance of the transcurrent kinematics. Extensional deformations could be interpreted as resulting from surficial stresses induced by a relative left-lateral transcurrent motions between the CO and CR with a diverging component [Fig. 17(b)].

The interpretation of the IV as a sort of basin carried piggyback above deeper transpressional faults and the possibility of deformation of the filling sequence can find a similarity in other regions characterized by normal faulting parallel to the chain and synchronous with the orogenesis. An example is the onlapping sequence of a piggyback basin in northwestern Canada which was deformed when deeper faulting progressed (Cook and Clark, 1990), or the normal faulting developed as a response to the thrust-related uplift in the south-central Brooks Range of Alaska (Gottschalk and Oldow, 1988). Here the normal faults provided local structural control on the locus of the sedimentation which was synchronous with thrusting. In all cases longitudinal valleys parallel to the fold and thrust belt are the result. Our model of the IV introduces a kinematic explanation which is intermediate between the classical piggyback longitudinal basin and the divergent wrench tectonics of Wilcox *et al.* (1973) and which could be tested in similar geological settings as, for example, the Central Valley of Chile (Beck *et al.*, 1986).

5.3. Regional kinematics

The CR represents a basement crustal block which is being uplifted and pushed toward NNE as a consequence of the oblique convergence between the Nazca and the South America plates. The relative motions of this block with respect to the adjacent sectors can explain the right-lateral and left-lateral shear component respectively observed in the CR and in the IV since Late Pleistocene. The scales of the deformations are different in the two fault belts. Total slips measured on latest Pleistocene–Holocene fault planes are of the order of meters to some tens of meters in the IV. Latest Pleistocene–Holocene total fault slips amount to an order of tens to some hundreds of meters in the CR (Tibaldi and Ferrari, 1992). This implies that the CR block is moving to NNE with respect to the stable South America at a higher relative speed than the CO. This kinematic model is consistent with the regional tectonics of Northern Andes (North Andean Block) where the right-lateral strike–slip fault system of the eastern CR continues in the Colombia and Venezuela territory and the left transtensional fault system of the IV continues northward along the fault zone of the Cauca Valley (MacDonald, 1980; Tibaldi and Ferrari, 1990; Soulas *et al.*, 1991). All the North Andean Block is presently escaping toward NNE due to the presence of convenient line of weakness and the oblique convergence between the continental and oceanic crust. The relative escape rate is higher for the NE Andean block, bounded between the two shear zones, with respect to the NW Andean block, bounded between the trench and the left-lateral shear zone. The Pleistocene change from right-lateral to left-lateral motions along the IV could correspond to a regional variation in the motion velocity vectors toward NNE of the NE and NW Andean blocks.

6. CONCLUSIONS

The structural evolution of the IV was studied by integration of meso- and microtectonic observations based on published and unpublished stratigraphic data. The oldest outcropping rocks, represented by continental deposits of Miocene age, are involved in a compressional phase of latest Miocene age which produced cylindrical east-vergent folds with NNE–SSW axis and parallel pure reverse faults. Structural trends were parallel to the Cordilleras ones.

After this tectonic phase the western IV was filled with volcanic rocks, dated at 6 Ma which was affected by NNE right-lateral strike–slip faults. This deformation could have been contemporaneous with the early Pleistocene N–S folds found in the southern IV (Latacunga area). A simple shear mechanism of deformation is suggested for this phase.

Lacustrine, fluvial and volcanic rocks were deposited in the IV between early and middle Pleistocene. During late Pleistocene they were subsequently affected by en-echelon reverse and strike–slip faults and E–W folds following an N–S trending $\sigma 1$. Deformation occurred within a narrow NNE–SSW belt along the

central-western part of the IV and suggests a transpressional mechanism with an inverted sense of motion.

Volcanic activity and fluvio-lacustrine sedimentation lasted until the Holocene. Between the end of Pleistocene and the Present en-echelon N–S pure normal and NNE–SSW left- lateral normal faults developed especially along a NNE–SSW belt in the central-western part of the IV. Extensional deformations occurred in response to an E–W trending $\sigma 3$. This phase seems to be controlled by a transtensional mechanism of deformation.

Considering the development of NNE–SSW transcurrent faults in recent times also in the Cordilleras and the presence of a large tectonic suture buried under the deposits of the IV, we suggest that the last compressional and extensional deformations may be explained by a relative left-lateral motion between the two Cordilleras. A converging component produced the transpressional pulse, while a diverging component resulted in the transtensional regime of the latest Pleistocene–Holocene pulse. In this frame the IV resembles a piggyback basin lying between the two uplifting ridges of the CO and CR.

Acknowledgments—We thank M. Coltelli and G. Pasquarè for field co-operation. We also thank ELC- Electroconsult society, Milan, for logistical facilities provided in the initial part of the field work. Reviews from W. Jacoby, K. J. Reutter and two anonimous referees of JG were very helpful. The research was partially supported by Ph.D. grants from Ministero Italiano della Pubblica Istruzione.

REFERENCES

Baldock J. W. (1982) Geologia del Ecuador (Boletin de la explicaciòn y mapa geologico de la Republica del Ecuador, escala 1:1,000,000). Direcciòn General de Geologia y Minas, Quito, 71 pp.

Baldock J. W. (1985) The Northern Andes: a review of the Ecuadorian Pacific Margin. In *The Ocean Basins and Margins* (A. E. M. Nairn, G. F. Stelhi and S. Uyeda, eds), Vol. 7A, (The Pacific Ocean), pp. 181–217. Plenum Press, New York.

Barberi F., Coltelli M., Ferrara G., Innocenti F., Navarro J. M. and Santacroce R. (1988) Plio-Quaternary volcanism in Ecuador. *Geol. Mag.* **125(1),** 1–14.

Beck M. E., Drake R. E. and Butler R. F. (1986) Paleomagnetism of Cretaceous volcanic rocks from central Chile and implications for the tectonics of the Andes. *Geology* **14,** 132–136.

Bonhomme M. G., Lavenu A., Noblet C., Dugas F., Eguez A. and Vivier G. (1990) Nouvelles datations K/Ar sur des roches volcaniques tertiaires et quaternaires des bassins continentaux introcordillerains d'Equateur. *Proc. Int. Symp Andean Geodynamics*, Grenoble, France, p. 283.

Bristow, C. R. and Hoffstetter R. (1977) *Lexique stratigraphique international: Ecuador.* Vol. 5, 2nd edn. Centre National de la Recherche Scientifique, Paris.

Carey E. (1979) Recherche des directions principales de contraintes associees au jeu d'une populiation des failles. *Rev. Geogr. Phys. Geol. Dyn.* **21(1),** 57–66.

Coltelli M. and Tibaldi A. (1992) Evoluzione geologico-strutturale di una direttrice principale antiandina: la Valle del Chota, Equador. Rend. Acc. Naz. Lincei.

Cook F. and Clark E. (1990) Middle Proterozoic piggyback basin in the subsurface of northwestern Canada. *Geology* **18,** 662–664.

Cross T. A. and Pilger R. H. (1982) Controls of subduction geometry, location of magmatic arcs and tectonics of arcs and back-arc regions. *Geol. Soc. Am. Bull.* **93,** 545–562.

Daly M. C. (1989) Correlations between Nazca/Farallon plate kinematics and forearc basin evolution in Ecuador. *Tectonics* **8, 4,** 769–790.

DGGM (Direcciòn General de Geologie y Minas) (1978) Mapa geologico del Ecuador, escala 1:100,000; hoya, 68, Ambato. Quito.

DGGM (Direcciòn General de Geologia y Minas) (1980a) Mapa geologico del Ecuador, escala 1:100,000; hoya 82, Ibarra. Quito.

DGGM (Direcciòn General de Geologie y Minas) (1980b) Mapa geologico del Ecuador, escala 1:100,000; hoya 67, Latacunga. Quito.

DGGM (Direcciòn General de Geologia y Minas) (1982) Mapa geologico del Ecuador, escala 1:25,000; hoya Guayllabamba. Quito.

Feininger T. (1977) Mapa gravimetrico Bouguer del Ecuador (1:1,000,000). Quito: Instituto Geografico Militar.

Feininger T. and Bristow C. R. (1980) Cretaceous and Paleogene geologic history of coastal Ecuador. *Geologische Rundschau* **69,** 849–874.

Feininger T. and Seguin M. K. (1983) Simple Bouguer gravity anomaly field and the inferred crustal structure of continental Ecuador. *Geology* **11,** 40–44.

Ferrari L. and Tibaldi A. (1989) Seismotectonics of North-Eastern Ecuadorian Andes. Annales Geophisicae, special issue on EGS XIV General Assembly, 39 (abstract).

Ferrari L. and Tibaldi A. (1992) Recent and active tectonics of the north-eastern Ecuadorian Andes. *J. Geodynamics* **15,** 39–58.

Gottschalk R. R. and Oldow J. S. (1988) Low-angle normal faults in the south-central Brooks Range fold and thrust belt, Alaska. *Geology* **16,** 395–399.

Hall M. L. and Wood C. D. (1985) Volcano-tectonic segmentation of Northern Ecuadorian Andes. *Geology* **13,** 203–207.

Hall M. L., Basabe P. and Yepes H. (1980) Estudio de las fallas tectonicas y la actividad microsismica del Valle Interandino entre Pastocalkle y Ambato. *Politecnica, Monografia de Geologia* **V, 2,** 57–78.

Henderson W. G. (1979) Cretaceous to Eucene volcanic arc activity in the Andes of northern Ecuador. *J. Geol. Soc., London* **136,** 367–378.

Juteau T., Megard F., Raharison L. and Whitechurch H. (1977) Les assemblage ophiolitique de l'occident equatorien: nature petrographique et position strucurale. *Boll. Soc. Geol. France* **XIX** No. 5, 1127–1132.

Lebras M., Megard F., Dupuy C. and Dostal J. (1987) Geochemistry and tectonic setting of pre-collision Cretaceous and Paleogene volcanic rocks of Ecuador. *Geol. Soc. Am. Bull.* **99,** 569–578.

Litherland M. and Aspden J. A. (1990) Evidence for pre-Cretaceous collision in the Ecuadorian Andes. *Proc. Int. Symp. Andean Geodynamics* Grenoble, France, pp. 199–201.

MacDonald W. (1980) Anomalous paleomagnetic directions in late Tertiary andesitic intrusions of Cauca depression, Colombian Andes. *Tectonophysics* **68,** 339–348.

Ori G. G. and Friend P. F. (1984) Sedimentary basins formed and carried piggyback on active thrust sheets. *Geolgy* **12,** 475–478.

Ori G. G., Roveri M. and Vannoni F. (1986) Plio-Pleistocene sedimentation in the Apenninic-Adriatic foredeep (central Adriatic Sea, Italy). In *Foreland Basins, International Association Sedimentologists Special Publication* (Allen P. and Homewood P., eds), Vol. 8, 183–198.

Pasquarè G., Tibaldi A. and Ferrari L. (1990) Relationships between plate convergence and tectonic evolution of the Ecuadorian active Thrust Belt. In *Critical Aspects of Plate Tectonic Theory* (Agusthithus S. S., ed.), pp. 365–387. Theophrastus Publications, Athens.

Pieri M. (1983) Three seismic profiles thorugh the Po Plain. In *Seismic Atlas of Structural Styles* (Bally A., ed.) Am. Ass. Petr. Geol. Studies Geol. **15,** 3.4.1–3.4.8.

Roperch P., Megard F., Laj C., Mourier T., Clube T. M. and Noblet C. (1987) Rotated oceanic blocks in western Ecuador. *Geophys. Res. Lett.* **14,** 558–561.

Sebrier M., Mercier J. L., Megard F., Laubacher G. and Carey- Gailhardis E. (1985) Quaternary reverse and normal faulting and the state of stress in the Central Andes of South Peru. *Tectonics* **4,** 739–780.

Soulas J. P., Eguez A., Yepes H. and Perez H. (1991) Tectonica activa y riesgo sismico en los Andes Ecuatorianos y el extremo sur de Colombia. *Bol. Geol. Ecuat.* **2,** 3–11.

Tibaldi A. (1990) Tettonica trascorrente e archi vulcanici anomali: studio di alcune aree chiave in Ecuador e Messico. Ph.D. Thesis, in Italian with English abstract, Università di Milano, 195 pp.

Tibaldi A. and Coltelli M. (1989) Structural setting and Plio-Quaternary tectonic evolution of Interandean Valley, Ecuador. Annales Geophisicae, EGS XIV General Assemby, 38–39 (abstract).

Tibaldi A. and Ferrari L. (1990) A wedge model for the Quaternary tectonics of the Andes of Ecuador. *Proc. Int. Symp. Andean Geodynamics*, Grenoble, France, 119–121.

Tibaldi A. and Ferrari L. (1992) Latest Pleistocene-Holocene tectonics of the Ecuadorian Andes *Tectonophysics.*

Wilcox R. E., Harding T. P. and Seely D. R. (1973) Basic wrench tectonics. *Am. Ass. Petr. Geol. Bull.* **57, 1,** 74–96.

Villalba F. (1981) Geologia del Cuaternario en la zona entre Chota y Ambuqui, provincias de Imbambura y Charchi. *Monografia de Geologia, Escuela Politecnica, Quito,* **6,**5, 37–84.

Zeil W. (1979) *The Andes, a Geological Review.* Gebruder Borntraeger, Berlin.